

Double quantum-well tunnel junctions with high peak tunnel currents and low absorption for InP multi-junction solar cells

Matthew P. Lumb, Michael K. Yakes, María González, Igor Vurgaftman, Christopher G. Bailey, Raymond Hoheisel, and Robert J. Walters

Citation: *Applied Physics Letters* **100**, 213907 (2012); doi: 10.1063/1.4722890

View online: <http://dx.doi.org/10.1063/1.4722890>

View Table of Contents: <http://scitation.aip.org/content/aip/journal/apl/100/21?ver=pdfcov>

Published by the [AIP Publishing](#)

Articles you may be interested in

[Impacts of ambipolar carrier escape on current-voltage characteristics in a type-I quantum-well solar cell](#)
Appl. Phys. Lett. **103**, 061118 (2013); 10.1063/1.4818510

[Improved photovoltaic effects in InGaN-based multiple quantum well solar cell with graphene on indium tin oxide nanodot nodes for transparent and current spreading electrode](#)
Appl. Phys. Lett. **102**, 031116 (2013); 10.1063/1.4789502

[Open-circuit-voltage enhancement of the III-V super-lattice solar cells under optical concentration](#)
AIP Conf. Proc. **1477**, 40 (2012); 10.1063/1.4753829

[Electron-beam-induced current and cathodoluminescence characterization of InGaAs strain-balanced multiquantum well photovoltaic cells](#)
J. Appl. Phys. **94**, 6341 (2003); 10.1063/1.1618924

[Effect of Be doping on the absorption of InGaAs/AlGaAs strained quantum-well infrared photodetectors grown by molecular-beam epitaxy](#)
Appl. Phys. Lett. **74**, 1570 (1999); 10.1063/1.123619



AIP | Journal of
Applied Physics

Journal of Applied Physics is pleased to
announce **André Anders** as its new Editor-in-Chief

Double quantum-well tunnel junctions with high peak tunnel currents and low absorption for InP multi-junction solar cells

Matthew P. Lumb,^{1,2} Michael K. Yakes,² María González,^{2,3} Igor Vurgaftman,² Christopher G. Bailey,² Raymond Hoheisel,^{1,2} and Robert J. Walters²

¹The George Washington University, 2121 I Street NW, Washington DC 20037, USA

²Naval Research Laboratory, Washington DC 20375, USA

³Sotera Defense Solutions, 2200 Defense Highway, Suite 405, Crofton, Maryland 21114, USA

(Received 30 March 2012; accepted 11 May 2012; published online 24 May 2012)

Lattice matched InAlGaAs tunnel junctions with a 1.18 eV bandgap have been grown for a triple-junction solar cell on InP. By including two InGaAs quantum wells in the structure, a peak tunnel current density of 113 A/cm² was observed, 45 times greater than the baseline bulk InAlGaAs tunnel junction. The differential resistance of the quantum well device is $7.52 \times 10^{-4} \Omega \text{ cm}^2$, a 15-fold improvement over the baseline device. The transmission loss to the bottom cell is estimated to be approximately 1.7% and a network simulation demonstrates that quantum well tunnel junctions play a key role in improving performance at high sun-concentrations. © 2012 American Institute of Physics. [<http://dx.doi.org/10.1063/1.4722890>]

Tunnel junctions (TJs), or Esaki diodes,¹ are an important component of multi-junction solar cells, connecting the subcells of a monolithic multi-junction stack in electrical series. For optimal performance, it is important that the TJ has a high enough peak tunnel current density not to impede the flow of photocurrent between the subcells, which can reach tens of A/cm² in sun-concentrator applications.² Also, the differential resistance of the tunnel diode should be as low as possible to minimize any voltage drop across the diode. A final consideration for solar cell applications is that the TJ should be as transparent as possible to light below the band gap of the cell directly above the TJ, both to minimize the filtering of the light to the cell beneath and also to minimize the possibility of photocurrent being produced by the TJ.³⁻⁵

In this work, we discuss the development of a tunnel junction designed to operate between the middle and bottom cells of an InP-based triple junction (3J) solar cell. InP-based multi-junction cells are a promising route to high conversion efficiencies in both terrestrial and extra-terrestrial environments, and there have been recent successes in developing component cells for the InP-based 3J.⁶ The optimum bandgap configurations for the 3J under different spectra were determined by Gonzalez *et al.*⁷ The middle cell bandgap derived from this work was chosen to be 1.18 eV, achieved using the lattice-matched quaternary In_{0.52}Al_{0.33}Ga_{0.15}As. A basic p⁺⁺/n⁺⁺ tunnel junction was produced using this material and compared to an identical structure containing a pair of lattice-matched In_{0.53}Ga_{0.47}As quantum wells, providing much more efficient interband tunneling. Similar structures grown by other authors have been shown to exhibit very high tunnel currents and peak to valley ratios (PVR) in the past.^{8,9} In this work, however, we examine the trade-off in the improved tunneling characteristics and the increased transmission loss using the quantum wells compared to the bulk TJ. Using a combination of IV characterization and modeling, the relative performance of the quantum well TJ and the bulk TJ was measured, with the quantum well tunnel junction (QWTJ) demonstrating a greater than 45-fold increase in the peak tunnel current and a

greater than 15-fold reduction in the differential resistance, with only a small impact on the transparency.

To evaluate the performance of the QWTJ versus a baseline device, two test structures were fabricated, one of which contained the QWTJ structure and the other contained the conventional bulk TJ structure. The device structures are summarized in Figure 1. The structures were grown using solid source molecular beam epitaxy. Each tunnel junction is surrounded by a 1500 Å $2 \times 10^{17} \text{ cm}^{-3}$ Si-doped (n-type) In_{0.53}Ga_{0.47}As buffer layer beneath and a 1500 Å

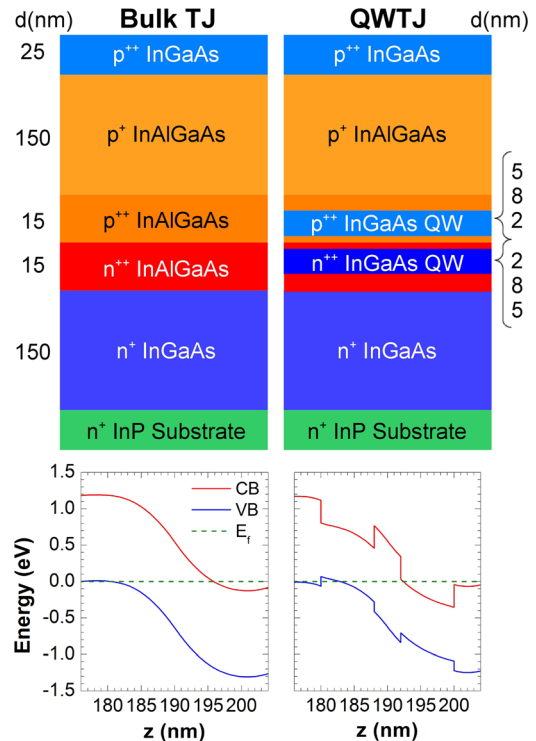


FIG. 1. A schematic diagram of the baseline bulk InAlGaAs TJ structure (left) and the QWTJ structure, incorporating two 80 Å InGaAs QWs (right). Calculated equilibrium band diagrams for the junction region of the two structures are shown (bottom).

$2 \times 10^{17} \text{ cm}^{-3}$ Be-doped (p-type) $\text{In}_{0.52}\text{Al}_{0.33}\text{Ga}_{0.15}\text{As}$ buffer layer above. These buffer layers were chosen to resemble the base and emitter regions of InAlGaAs and InGaAs middle and bottom cells in a 3J architecture. A 250 \AA $1 \times 10^{19} \text{ cm}^{-3}$ Si-doped $\text{In}_{0.53}\text{Ga}_{0.47}\text{As}$ cap layer was used to achieve an Ohmic contact to the front surface, and all the structures were grown on n-type InP wafers. The baseline bulk TJ has 150 \AA $\text{In}_{0.52}\text{Al}_{0.33}\text{Ga}_{0.15}\text{As}$ $1 \times 10^{19} \text{ cm}^{-3}$ Si-doped and $1 \times 10^{19} \text{ cm}^{-3}$ Be-doped layers. The QWTJ device has two 80 \AA QWs separated by a 40 \AA $\text{In}_{0.52}\text{Al}_{0.33}\text{Ga}_{0.15}\text{As}$ barrier and with 50 \AA $\text{In}_{0.52}\text{Al}_{0.33}\text{Ga}_{0.15}\text{As}$ barriers either side, and the QWTJ device is designed so that the total thickness and doping are identical to the bulk TJ. The wafers were processed into circular devices with a mesa diameter of 1 mm and the current voltage characteristics were measured using a four point probe technique.

The equilibrium band structure of the devices was calculated using semiconductor band-solver software developed at the Naval Research Laboratory. The software numerically solves Poisson's equation in one dimension for a given layer structure, using band parameters taken from Vurgaftman *et al.*¹⁰ The band diagrams for the bulk TJ and QWTJ are shown in Figure 1. The QWTJ calculation assumed the bulk properties of InGaAs within the quantum wells which provide a good first approximation to the band structure of the QWTJ. However, quantum confinement effects modify the density of states in the QW regions and, strictly speaking, need to be accounted for, which will be the subject of further study.

The electrical characteristics of representative diodes of the bulk TJ and QWTJ are shown in Figure 2. The bulk TJ demonstrated a clear negative differential resistance (NDR) region, with a peak tunnel current density of 2.52 A/cm^2 and a peak to valley ratio of 4.8. Assuming a typical triple junction 1-sun short circuit current density of 15 mA/cm^2 , the peak tunnel current density corresponds to a concentration ratio (CR) of approximately 170 suns. The differential resistance of the tunnel diode was found to be $1.15 \times 10^{-2} \Omega \text{ cm}^2$. In comparison, the QWTJ demonstrated a much higher peak tunnel current density of 112.9 A/cm^2 , a factor of approximately 45 greater than the bulk TJ. In order to see the NDR

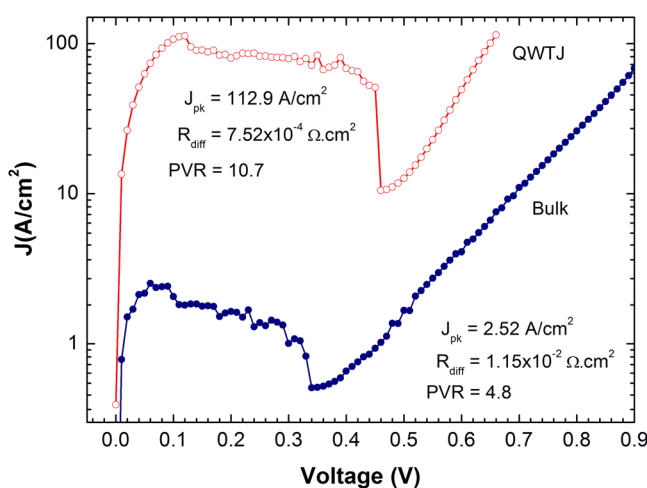


FIG. 2. A semi-log plot of current density versus voltage for the bulk TJ and the QWTJ measured using a four-point-probe technique.

in the two devices clearly, the IV curves are presented in Figure 2 on semi-log axes. The equivalent concentration of this current is approximately 7500 suns, which far exceeds the requirements for terrestrial concentration applications. A small differential resistance is extremely important for minimizing voltage losses in multi-junction solar cells, and the QWTJ exhibited a differential resistance of $7.52 \times 10^{-4} \Omega \text{ cm}^2$, which is a factor of 15.3 lower than the bulk diode. The PVR of the QWTJ was 10.7, and it is believed that this figure can be improved through further optimization of the barrier and well thicknesses.

The proposed mechanism for improving the tunneling characteristics of the diode is the efficient tunneling via the confined electron and hole energy levels of the quantum wells.⁹ Using bulk materials of a narrower bandgap, such as lattice-matched InGaAs, is well known to improve the resonant interband tunneling probability⁵ and high peak tunnel currents have been demonstrated using InGaAs TJs.¹¹ However, the benefit of the InGaAs QWs with wider bandgap barriers compared to a bulk InGaAs TJ is that efficient tunneling can be achieved with a much smaller impact on the transparency of the diode. It is important that the TJ is transparent to light lower in energy than the $\text{In}_{0.52}\text{Al}_{0.33}\text{Ga}_{0.15}\text{As}$ middle cell bandgap to minimize the filtering of light to the bottom cell. To approximate the absorption in the double QWTJ compared to bulk InGaAs beyond the middle cell bandgap, the absorption coefficient was calculated using the analytical solution to the finite square well problem in the effective mass approximation and in the absence of an electric field. This gives a rough estimate of the absorption coefficient and energy level structure of each well, although in reality the electric field across the wells significantly modifies the envelope wavefunctions and confined energies.¹² The confined energy levels of the quantum wells are displayed in the inset to Figure 3. The density of states was calculated using the familiar two dimensional density of states expression and the absorption coefficient then calculated using the overlap integrals deduced from the solution of the finite QW problem and the interband momentum matrix elements. For simplicity, the Coulombic attraction of the

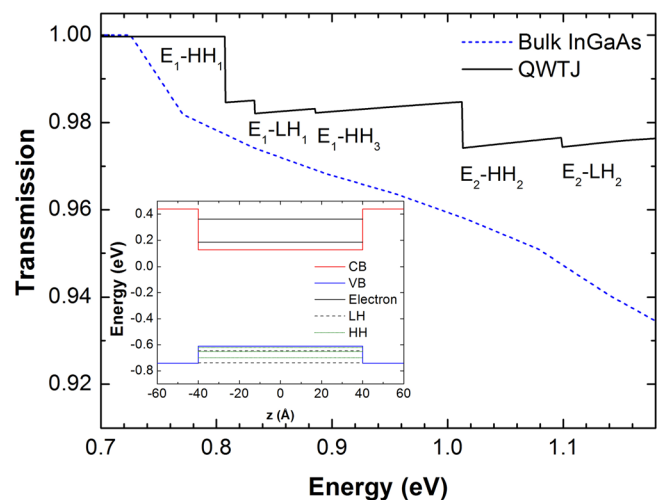


FIG. 3. The calculated transmission of the double QW region of the QWTJ compared to the same thickness of bulk InGaAs. The inset shows the confined energy levels in the InGaAs quantum well.

electrons and holes and broadening mechanisms were neglected. A more detailed description of the absorption calculation can be found in, for example, Ref. 13. The absorption calculated in this way can be seen as an upper limit, as the significant electric field across the QW region reduces the overlap integral of the electron and hole wavefunctions, thereby weakening the absorption. Therefore, the actual transmission losses during operation in the solar cell may be smaller than the estimate from this simple QW model.

The transmission of light below the InAlGaAs bandgap is shown in Figure 3 for both the QWTJ and bulk InGaAs. In the QWTJ case, the transmission was calculated using a transfer matrix technique, which takes into account the multiple reflections at the well/barrier interfaces, although the low index contrast of the layers results in a very small effect. The layer structure was two 80 Å QWs separated by a 40 Å InAlGaAs barrier and surrounded by two 50 Å InAlGaAs barriers, as shown in Figure 1. The substrate and ambient layers were assumed to be InAlGaAs also, to avoid the complications of multiple reflections at the front and rear surfaces of the structure. The real part of the refractive index for the QW layers was assumed to be that of bulk InGaAs. The transmission is compared to the single pass transmission through 300 Å of bulk InGaAs calculated using the Beer-Lambert law.

Results show that the transmission through the QWTJ is attenuated by approximately 1% per well above the lowest energy confined state of the well, and as shown in Figure 3 the transmission in the QWTJ is significantly greater than a bulk InGaAs TJ of the same overall thickness. This is important when considering the use of these structures within the 3J device. The power density contained in the ASTM AM1.5g spectrum between the energies of 0.74–1.18 eV is 165.8 W/m², and for the baseline InAlGaAs TJ it is assumed that all this power is transmitted through the junction region of the TJ. In the case of bulk InGaAs, 3.9% of the available light in this spectral region is absorbed. However, with the QWTJ only 1.7% of the light in this spectral band is absorbed. Even though the effect is reduced, the absorption in the QWs does still create a loss mechanism for the 3J solar cell. However, as discussed earlier, this simple QW model gives an upper limit to the transmission losses which may be lower in a real device. Furthermore, by using InAlGaAs QWs with a wider bandgap, it may be possible to lower the trade off in peak tunnel current and absorption.

To evaluate the trade-off in the transparency and differential resistance of the bulk and QWTJ structures, we used a network simulation of an idealized 3J solar cell with bandgaps of 1.74 eV, 1.18 eV, and 0.74 eV. A similar approach to Steiner *et al.*¹⁴ was employed and a schematic layout of the network simulation is shown in the inset to Figure 4. The simulation was split into nine illuminated components and one shaded component, each with an area of 1×10^{-6} cm², forming a cross-section between a grid finger and the halfway point of two grid fingers. Any voltage drop along the direction of the grid finger was neglected, allowing the network to extend only in one direction. The saturation current of the subcells was estimated from the radiative recombination limit⁷ and values of 7.5×10^{-27} A/cm², 8.9×10^{-18} A/cm², and 8.9×10^{-11} A/cm² were used for the top, middle, and bottom cells, respectively, assuming a temperature of 300 K.

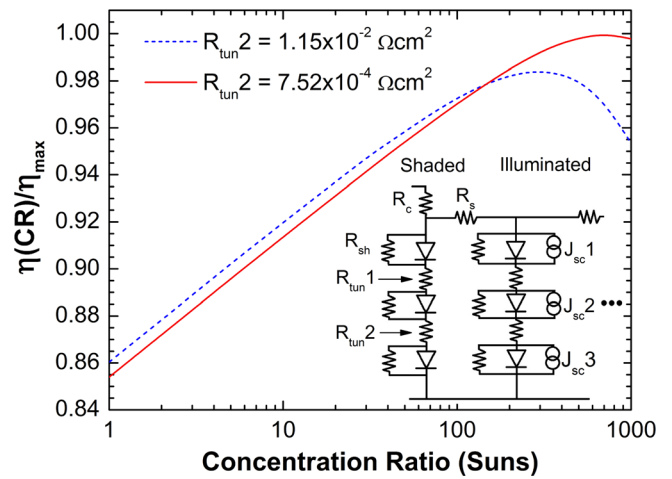


FIG. 4. Calculated values of normalized efficiency as a function of the CR for idealized 3J devices using the bulk (dotted blue line) and QW (solid red line) tunnel junctions. The inset shows a schematic of the network simulation layout.

The solar cell with the bulk TJ was chosen to be perfectly current matched and the short circuit current density for each sub-cell was arbitrarily chosen to be 15 mA/cm² under one sun conditions. We assumed that there was a linear relationship between the J_{sc} of the subcells and the solar CR. Each cell had a shunt resistance of 1×10^8 Ω cm², the spreading resistance of the top of the cell was assumed to be 200 Ω/□ and the contact resistance used a value of 3×10^{-6} Ω cm². The tunnel diodes were represented as resistors with the measured values of differential resistance from the bulk and QWTJ structures. This method allows a direct comparison of the differential resistance on the solar cell efficiency, but obviously does not take in to account the non-linearity of the tunnel diode. The differential resistance of the TJ between the first and second sub-cells was fixed at 1×10^{-4} Ω cm². To account for the absorption loss with the QWTJ, the short circuit current of bottom cell was reduced by 1.7%, making the 3J overall bottom cell limited.

Figure 4 shows the simulated efficiency of the 3J cells normalized to the peak efficiency. At low concentrations, the filtering of the light to the bottom cell reduces the conversion efficiency of the 3J with the QWTJ by approximately 0.7% relative to the baseline TJ, due to the bottom cell limiting the current. However, for concentrations above 140 suns the QWTJ device becomes more efficient due to the lower resistive loss, and at 1000 suns the QWTJ device has approximately a 4.4% higher efficiency relative to the bulk device. In reality, once the concentration ratio exceeds approximately 170 suns, the increase in efficiency of the QWTJ will be greater still due to the photocurrent exceeding the peak tunnel current of the bulk TJ. This will cause the bulk TJ to pass current in the thermal diffusion mode, thereby incurring a much larger voltage drop.¹⁴ The small absorption loss in the QWTJ device therefore has only a very small impact on the performance at high concentration due to the much smaller resistive loss.

In conclusion, we have demonstrated a quantum well tunnel junction structure which can be used to improve the performance of a multi-junction solar cell. By incorporating two InGaAs QWs, a peak tunnel current of 113 A/cm² was

observed, which was a 45-fold increase over the baseline InAlGaAs TJ, and a differential resistance of $7.52 \times 10^{-4} \Omega \text{ cm}^2$, which was a 15.3-fold improvement over the baseline device. The increase in the spectral power absorbed in the QW region is estimated to be about 1.7%, which is significantly smaller than a bulk InGaAs TJ which absorbs 3.9%. This yields a device which can far surpass the electrical performance of the conventional tunnel junction structure at high concentrations with minimal transmission loss. We believe that the design can be further optimized to improve the transparency whilst still achieving extremely high peak tunnel currents by tailoring the QW depth and the barrier thickness. In addition to the role in developing multi-junction solar cells on InP, analogous QWTJs could improve the performance of the more established 3J devices based on Ge or GaAs substrates.

The author would like to thank Woojun Yoon, Chaffra Affouda, and Joe Tischler for valuable contributions to this work. This work was supported by the Office of Naval Research.

¹L. Esaki, *Phys. Rev.* **109**(2), 603 (1958).

²F. Dimroth, *Phys. Status Solidi C* **3**, 373 (2006).

³M. Yamaguchi, *Sol. Energy Mater. Sol. Cells* **75**(1–2), 261 (2003).

⁴M. Yamaguchi, K.-I. Nishimura, T. Sasaki, H. Suzuki, K. Arafune, N. Kojima, Y. Ohsita, Y. Okada, A. Yamamoto, T. Takamoto, and K. Araki, *Sol. Energy* **82**(2), 173 (2008).

⁵J. F. Wheeldon, C. E. Valdivia, A. W. Walker, G. Kolhatkar, A. Jaouad, A. Turala, B. Riel, D. Masson, N. Puetz, S. Fafard, R. Arès, V. Aimez, T. J. Hall, and K. Hinzler, *Prog. Photovoltaics* **19**(4), 442 (2011).

⁶M. S. Leite, R. L. Woo, W. D. Hong, D. C. Law, and H. A. Atwater, *Appl. Phys. Lett.* **98**(9), 093502 (2011).

⁷M. González, N. Chan, N. J. Ekins-Daukes, J. G. J. Adams, P. Stavrinou, I. Vurgaftman, J. R. Meyer, J. Abell, R. J. Walters, C. D. Cress, and P. P. Jenkins, in *Proceedings of SPIE, Physics and Simulation of Optoelectronic Devices XIX*, San Francisco, edited by B. Witzigmann, F. Henneberger, Y. Arakawa, and A. Freundlich (SPIE, 2011).

⁸S. Sutar, Q. Zhang, and A. Seabaugh, *IEEE Trans. Electron Devices* **57**(10), 2587 (2010).

⁹H. H. Tsai, Y. K. Su, H. H. Lin, R. L. Wang, and T. L. Lee, *IEEE Electron Device Lett.* **15**(9), 357 (1994).

¹⁰I. Vurgaftman, J. R. Meyer, and L. R. Ram-Mohan, *J. Appl. Phys.* **89**(11), 5815 (2001).

¹¹G. M. Cohen, D. Ritter, and C. Cytermann, *Electron. Lett.* **31**(17), 1511 (1995).

¹²D. A. B. Miller, D. S. Chemla, T. C. Damen, A. C. Gossard, W. Wiegmann, T. H. Wood, and C. A. Burrus, *Phys. Rev. B.* **32**(2), 1043 (1985).

¹³J. Singh, *Electronic and Optoelectronic Properties of Semiconductor Structures* (Cambridge University Press, Cambridge, 2003).

¹⁴M. Steiner, W. Guter, G. Peharz, S. P. Philipps, F. Dimroth, and A. W. Bett, *Prog. Photovoltaics* **20**(3), 274 (2011).